中国物理 B
Chinese Physics
Chinese Physics B

Structural response of aluminum core-shell particles in detonation environment

Qing-Jie Jiao(焦清介), Qiu-Shi Wang(王秋实), Jian-Xin Nie(聂建新), Hong-Bo Pei(裴红波)
Citation: Chin. Phys. B . 2019, 28(8): 088201 . **doi:** 10.1088/1674-1056/28/8/088201
Journal homepage: http://cpb.iphy.ac.cn; http://iopscience.iop.org/cpb

What follows is a list of articles you may be interested in

Acoustic characteristics of pulse detonation engine with ellipsoidal reflector

Yang Kang(康杨), Ning Li(李宁), Chun-Sheng Weng(翁春生), Chuan-Wei Wang(王传位)
Chin. Phys. B . 2018, 27(10): 104703 . **doi:** 10.1088/1674-1056/27/10/104703

Three-dimensional detonation cellular structures in rectangular ducts using an improved CESE scheme

Yang Shen(沈洋), Hua Shen(申华), Kai-Xin Liu(刘凯欣), Pu Chen(陈璞), De-Liang Zhang(张德良)
Chin. Phys. B . 2016, 25(11): 114702 . **doi:** 10.1088/1674-1056/25/11/114702

Critical deflagration waves leading to detonation onset under different boundary conditions

Lin Wei, Zhou Jin, Fan Xiao-Hua, Lin Zhi-Yong
Chin. Phys. B . 2015, 24(1): 014701 . **doi:** 10.1088/1674-1056/24/1/014701

Particle path tracking method in two-and three-dimensional continuously rotating detonation engines

Zhou Rui, Wu Dan, Liu Yan, Wang Jian-Ping
Chin. Phys. B . 2014, 23(12): 124704 . **doi:** 10.1088/1674-1056/23/12/124704

Existence of a Hartmann layer in the peristalsis of Sisko fluid

Saleem Asghar, Tayyaba Minhas, Aamir Ali
Chin. Phys. B . 2014, 23(5): 054702 . **doi:** 10.1088/1674-1056/23/5/054702

Structural response of aluminum core–shell particles in detonation environment*

Qing-Jie Jiao(焦清介)[1], Qiu-Shi Wang(王秋实)[1], Jian-Xin Nie(聂建新)[1,†], and Hong-Bo Pei(裴红波)[2]

[1] *State Key Laboratory of Explosion Science and Technology, Beijing Institute of Technology, Beijing* 100081, *China*
[2] *China Academy of Engineering Physics, Institute of Fluid Physics, Mianyang* 621900, *China*

(Received 21 May 2019; revised manuscript received 13 June 2019; published online 25 July 2019)

Natural aluminum particles have the core–shell structure. The structure response refers to the mechanical behavior of the aluminum particle structure caused by external influences. The dynamic behavior of the structural response of aluminum core–shell particles before combustion is of great importance for the aluminum powder burning mechanism and its applications. In this paper, an aluminum particle combustion experiment in a detonation environment is conducted and analyzed; the breakage factors of aluminum particles shell in detonation environment are analyzed. The experiment results show that the aluminum particle burns in a gaseous state and condenses into a sub-micron particle cluster. The calculation and simulation demonstrate that the rupture of aluminum particle shell in the detonation environment is mainly caused by the impact of the detonation wave. The detonation wave impacts the aluminum particles, resulting in shell cracking, and due to the shrinkage-expansion of the aluminum core and stripping of the detonation product, the cracked shell is fractured and peeled with the aluminum reacting with the detonation product.

Keywords: aluminum core–shell particles, structural response, aluminum combustion, aluminized explosives

PACS: 82.33.Vx, 47.40.Rs, 47.70.Pq, 65.80.–g **DOI:** 10.1088/1674-1056/28/8/088201

1. Introduction

Aluminum powder can greatly increase the potential energy of composite energetic material, such as explosives and propellants.[1–4] However, much of the potential cannot be released due to incomplete combustion. The study of aluminum powder combustion theory in detonation environment is of great significance to solve the above problem and enrich the theoretical model of metal powder combustion.

Natural aluminum particles have the core–shell structure.[5] The structure response is the mechanical behavior of the aluminum particle structure caused by external influences. An aluminum ignition and combustion occurs after oxide shell separation, so the response mechanism of the core–shell structure of aluminum particle before ignition is the focus of aluminum powder combustion theory. The study of core–shell structural response of aluminum particle under slow heating conditions is conducted in detail.

Eisenreich[6] researched the slow thermal response of aluminum powder for certain size ranges with different stages of aluminum oxidation being observed. His conclusions were supported and referenced by other scholars, such as Hasani and Korshunov.[7–9] Further, Eisenreich[10] noted that the alumina layer has a phase change in oxidation, but there was no quantitative correlation between the dynamic changes of phase transformation and oxidation.

Dreizin[11] studied Al particle combustion in air using a pulsed micro-arc discharge. He found that the Al particle combustion corresponds to different temperatures, internal particle compositions, and flame shapes. Trunov[12,13] also noted that the growth of the crystal phase change caused by the micron aluminum oxide layer is directly related to the aluminum oxidation behavior.

Trunov[14,15] proposed a reaction model for the aluminum slow weighting process as affected by the shell phase transformation for micro-aluminum. The phase change of the alumina was divided into four stages. For stage 1, the reaction temperature is less than 800 K, the natural amorphous state of the alumina shell grows, the crystal shape changes to γ-Al_2O_3, and the oxide layer thickens. During stage 2, between 800 K and 910 K, the transfer rate of the active material through the oxide layer increases, further promoting the phase change. At stage 3, between 910 K to 1320 K, the γ-Al_2O_3 oxide layer thickens and changes to θ-Al_2O_3 and then α-Al_2O_3. For stage 4, the layer continues to change to α -Al_2O_3 and the thickness grows further.

Bradstant[16] studied the slow oxidation behavior of micro/nano aluminum powder in a CO_2 atmosphere. The maximum reaction temperature was 1250 °C and the results showed that the aluminum of less than 3 μm was oxidized completely. Using scanning electron microscopy (SEM), the oxidation products were characterized and an alumina hollow shell was observed. Combining energy dispersive spectrometer (EDS) analysis and phase characterization, the results showed that when the temperature of the thermal analysis in-

*Project supported by the National Natural Science Foundation of China (Grant No. 11772058).
†Corresponding author. E-mail: niejx@bit.edu.cn
© 2019 Chinese Physical Society and IOP Publishing Ltd

creased from 600 °C to 1000 °C, the carbon content of the solid phase also began to increase and then decrease. It is thought that this was the result of Al and CO_2 generating Al_2OC and Al_4O_4 C. Liu[17] did similar research and established the "eruption model".

Researchers also studied the combustion of aluminum particles. Glassman[18,19] first suggested that the metal particle burning was similar to droplet combustion, with the ignition depending on the melting and boiling point of the metal and oxide. He speculated that the stable aluminum combustion condition was melted alumina when the reaction temperature reached the boiling point of aluminum.

Further research confirmed the model proposed by Glassman.[20,21] Olsen[22] found that during the combustion, the generated liquid alumina would gather on the surface of particles, forming an alumina cap. Allen[23] studied nano-aluminum powder under high temperature combustion heat, verifying the Altman hypothesis. But previous research has also shown that the burning of aluminum began before the temperate reached the boiling point when the shell burst.[24] The reason for this may be different temperature and pressure environments[25] or mechanical stresses.[26]

In summary, the previous research focused on the structure response of aluminum particle in the thermal analysis (below 1500 K), and the combustion model of aluminum particles in the high temperature combustion environment (above 3000 K and below 10 MPa). However, the investigation on aluminum particle combustion in detonation environment (above 3000 K and more than 5 GPa) is deficient, which is significantly important to increase the efficiency of aluminum particle combustion. The purpose of this paper is to understand the mechanism of the structural response of aluminum core–shell particles in detonation environment.

2. Aluminum combustion experiment in detonation environments

2.1. Detonation experiment design

Table 1 shows the formulas of detonation test. Two kinds of aluminized explosive formula were designed; 2,4,6-trinitrotoluene (TNT) and octogen (HMX) were mixed with aluminum powder at a mass ratio of 80:20 (according to the calculation, the TNT/Al reaction temperature is 3077 K, HMX/Al is 3305 K, and the boiling point of alumina is 3253 K, so one is higher and another is lower). The detonation experiment was conducted in a steel pressure vessel with a diameter of 300 nm, a thickness of 15 mm, a height of 200 mm, and a volume of 14 liters. The schematic is shown in Fig. 1.

Aluminum was mixed with explosive to form charges. Three kinds of micron aluminum powder were used with particle sizes of 10 μm, 30 μm, and 90 μm. The mass of each charge was 14.1 g with a diameter of 20 mm. The TNT's purity was more than 99% with an average particle size of 90 μm; the HMX was a plastic bonded explosive containing 4% binder with an average particle size of 80 μm.

Table 1. Formulas of detonation test.

ID No.	Mixture	Particle size/μm	Density/(g/cm^3)	Mass/g
A1	TNT/Al (80/20)	10+30	1.62	14.1
A2	TNT/Al (80/20)	30+90	1.62	14.1
A3	HMX/Al(80/20)	10+30	1.81	14.1
A4	HMX/Al(80/20)	30+90	1.81	14.1

Note: 10+30 means the weight ratio of 10-μm Al to 30-μm Al is 1:1.

The explosive was initiated by the #8 electric detonator and 2.2-g composition RDX/wax (95/5) booster. The booster and charge were glued together and the detonator was inserted into the booster hole. The red sample in Fig. 1 is the detonator, booster, and mixture, which was laterally placed in the center of the vessel through the detonator lead. In Fig. 2, the booster was black, which had the detonator hole, and the white part was the aluminum/explosive mixture. The detonation product included the solid product and the gas product. Only the solid product was retrieved and analyzed. It was baked for 1 hour at 60 °C before analysis.

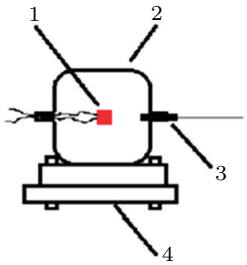


Fig. 1. The schematic diagram of detonation experiment. 1: Sample, 2: vessel, 3: sensor, 4: flange.



Fig. 2. The sample photograph (black part indicates the booster and white indicates the mixture).

2.2. Solid detonation product analysis

Solid detonation product is analyzed. The main solid detonation product is Al_2O_3. The appearance of the four formulas is similar. The typical SEM images of the products are shown in Fig. 3. There are two main types of product appearance. One is like that as shown in Fig. 3(a) with product recycled from the container walls, which does not have a regular

shape and is around several hundred micrometers in diameter (greater than the initial particle size of aluminum powder). From the enlarged drawing, it can be seen that there are many surface craters of different sizes. These products are formed due to the fact that the molten aluminum oxide has congealed on the metal container wall and the craters are due to collisions of other product particles at high speed.

The other one is like that as shown in Fig. 3(b). Unlike the Al burning product in the air,[16,17] the detonation product particle size is much smaller than the original. From the enlarged drawing in Fig. 3(b), sub-micron particles with size of 100 nm–200 nm are clustered on the surface coinciding with the mechanism of the aluminum powder gas reaction. The larger particle product may be formed by the cluster of many submicron particles.

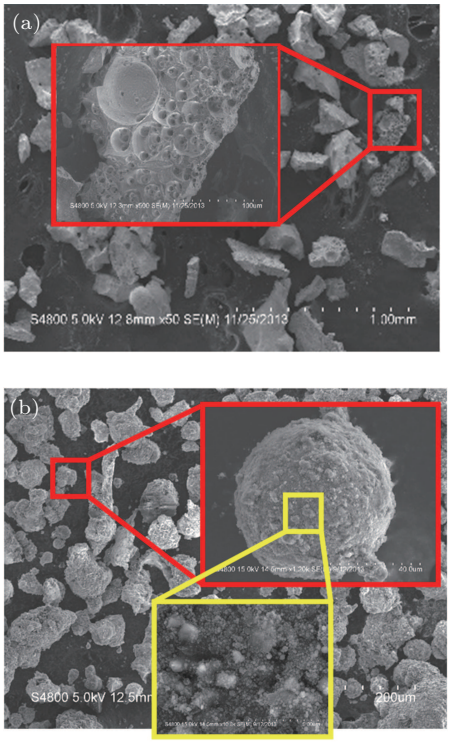


Fig. 3. The SEM image of solid detonation product.

The x-ray diffraction (XRD) results are shown in Fig. 4. The product crystallography analysis of the detonation products in Table 2 demonstrates that the percentage of unreacted aluminum is small, which is quite different from combustion. The numerical error is 2%. The source of the error is that small-sized crystalline phase materials in solid detonation products can cause the instrument fail to determine the type, which in turn leads to systematic errors.

Table 2. Crystal phase compositions of condensed detonation products.

ID No.	Al	Al_2O_3	Al_2OC	AlN	Diamond
A1	0	82	3	7	8
A2	5	71	4	11	9
A3	0	100	0	0	0
A4	2	96	2	0	0

The product photo shows that the aluminum particle burns in a gaseous state and condenses into a sub-micron particle cluster. The premise of the aluminum powder gas phase reaction is that the particle shell is broken, and then the core is exposed to the high temperature gas, vaporizing, burning, and condensing into a sub-micron particle cluster.

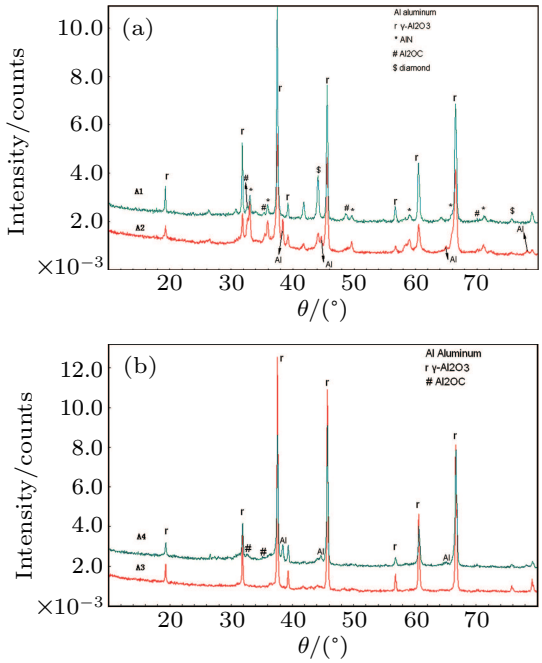


Fig. 4. XRD results of condensed detonation products: (a) TNT/Al; (b) HMX/Al.

3. The breakage factors analysis of aluminum particles shell in detonation environment

Combined with the literature and experimental results, the potential mechanism for the separation of aluminum core–shell particles in detonation environment is as follows.

(I) Thermal stress. The density of solid aluminum is 2.7 g/cm^3, and the density of liquid aluminum is 2.4 g/cm^3. Therefore, when the aluminum core is melted, its volume expands by 12%. The aluminum shell swells and ruptures due to internal tensile stress.

(II) Detonation wave. The detonation wave pressure is greater than 10 GPa in the aluminized explosive reaction zone. Such high pressure causes a large deformation of the aluminum powder, which makes alumina shell fail to crack, forming cracks on the surface of the aluminum.

In the detonation environment, high temperature and strong impact are present simultaneously, and the two factors should be considered comprehensively. By calculating the separation time required for the two methods, the main cause of the core–shell deconstruction in the detonation environment can be determined.

(III) Crystal transformation and phase transformation of alumina. Thermal analysis results[27,28] show that as the tem-

perature increases, the alumina changes from an amorphous state to γ and θ states, eventually forming a stable α state. When the crystal form of alumina changes, its density increases all the time, causing the volume of alumina to decrease, which causes the alumina to not completely cover the aluminum core, resulting in shell–core separation.

In summary, the crystal transformation and phase transformation of alumina are the main reasons for shelling in thermal analysis environment (300 °C–1100 °C); in the combustion reaction, thermal stress is the main reason; in the detonation environment, high temperature and strong impact are present simultaneously, and the two factors should be considered comprehensively. By calculating the separation time required for the two methods, the main cause of the core–shell deconstruction in the detonation environment can be determined.

3.1. The rupture time of thermal stress

The melting point of aluminum is 933 K.[29] TNT/Al (80/20) explosive detonation temperature is 3309 K by cast formula.[30] Taking 10-μm aluminum particles as an example, the time for the alumina shell and aluminum core rising to the melting point (t_{mel}) is calculated. t_{mel} can be treated as the time when the shell is ruptured by thermal stress

$$t_{\mathrm{mel}} = \frac{Q(x)}{P(x)}, \tag{1}$$

where $Q(x)$ is the amount of heat required to rise to the melting point of aluminum (in the unit of J), $P(x)$ is the endothermic power (in the unit of W), and x is the distance from the aluminum surface to the center (in the unit of m). When considering the phase change of substance,

$$Q(x) = (\Sigma C_{\mathrm{Vi}} \Delta T_{\mathrm{i}} + \Sigma \Delta H_{\mathrm{mi}}) \rho \frac{4}{3} \pi [R^3 - (R-x)^3], \tag{2}$$

where C_{Vi} is the specific heat capacity of different phases of the material (in the unit of J/kg·K), m is the mass of the substance (in the unit of kg), and ΔH_{m} is the substance enthalpy of phase change (in the unit of J/kg), and

$$P(x) = \frac{qS(x)}{x} = \frac{q \int_0^R 4\pi (R-X)^2 \mathrm{d}x}{x}, \tag{3}$$

where q is the heat flux (in the unit of W/m^2), and $S(x)$ is the heated area (in the unit of m^2).

According to Fourier's law

$$q = \lambda \frac{\Delta T}{x}, \tag{4}$$

where λ is the thermal conductivity of the substance, which is taken as 210 W/m·K for aluminum, and 18 W/m·K for alumina.

Bring the heat capacity, phase change enthalpy, and other parameters[29] into the formula, and t_{mel} can be calculated.

When the diameter of aluminum particle is 10 μm, the shell rises to 933 K for 0.013 ns and the core is 53.6 ns. The t_{mel} values for particles of other diameters are shown in Table 3.

Table 3. Heating time of different aluminum particle sizes reaching the aluminum melting point.

Diameter of aluminum particles /μm	2	10	30	90
t_{mel}/ns	5.9	53.6	248.2	1343.5

3.2. Breakage time of alumina shell by detonation wave

To investigate the mechanical response of aluminum particle in the detonation shock wave, the finite element software AUTODYN[31] is employed. The aluminum with core diameter of 10 μm and shell thickness of 20 nm is chosen for the study. The calculation model is shown in Fig. 5, where the core, shell, and TNT are labeled in blue, red, and green, respectively. Four gauge points are set, which are located at the axes of the explosive, aluminum edge, half radius, and core center.

The simulation model consists of TNT, aluminum, and alumina. The location of the detonation of the TNT is to the left of the surface. The relationship between pressure and the relative volume of the TNT product is as described by the Jones–Wilkins–Lee (JWL) state equation.[32] The constitutive equations of aluminum are described by the Von Mises model[33] and the constitutive equations of alumina are described by the Johnson–Holmquist (JH) model.[34]

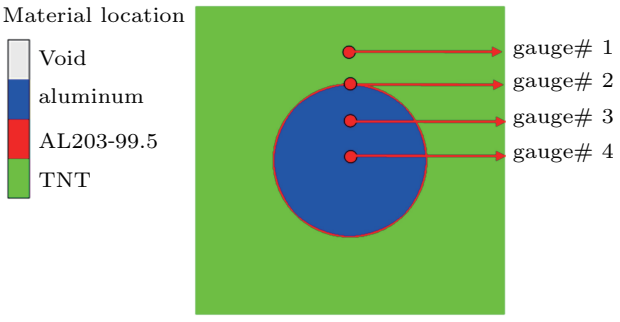


Fig. 5. The diagram of simulation model.

The detonation shock wave impacts the aluminum particle with a force of tens of GPa. The different mechanical properties of alumina and aluminum lead to different types of deformation: the alumina shell fails and fractures under the shock wave and the aluminum core experiences elastic-plastic deformation. Figure 6 shows the process of the detonation wave impacting on the particle.

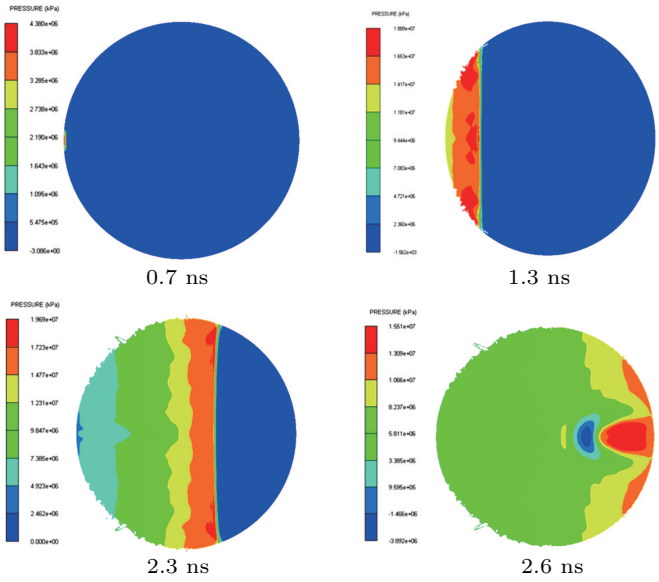


Fig. 6. The pressure nephogram of aluminum particles in different times.

Figure 7 shows the particle deformation and failure process. By analyzing the breakage of the shell, the most serious shock wave attack angle is 45° with the top and back also being damaged.

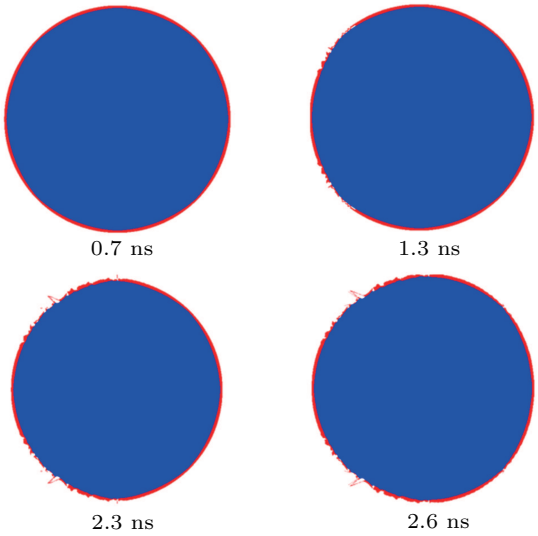


Fig. 7. Deformation and failure process of aluminum and alumina shell.

Based on this simulation, the shell breakage times for different particle sizes are obtained, and the results are shown in Table 4.

Table 4. The breakage time of alumina shell for different particle sizes.

Particle size/μm	2	10	30	90
Breakage time/ns	1.3	3.3	8.7	24.5

At the same particle size, the alumina shell breakage of the detonation wave impact is significantly less than t_{mel} caused by the thermal stress. Therefore, the rupture of the aluminum particle shell in the detonation environment is mainly caused by the impact of the detonation wave.

The velocity curves of four gauges are calculated, as shown in Fig. 8. The speed of the gauge points is extracted as 1488 m/s for gauge #1, 946 m/s for gauge #2, 975 m/s for gauge #3, and 927 m/s for gauge #4. Therefore, after the shell bursts, the detonation product moves faster than the aluminum and the edge speed is higher than the center; the outer aluminum will be peeled, which subsequently promotes core contact with the detonation product and burning.

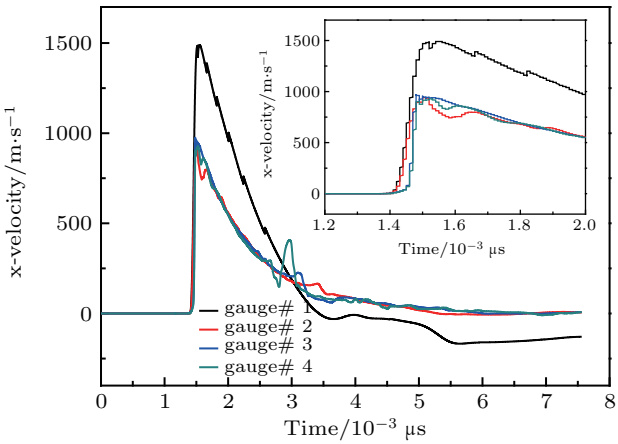


Fig. 8. The velocity curves of gauges.

4. Structure response stages of aluminum core–shell particles in detonation environment

According to the detonation product and simulation results, the structure response of aluminum particle can be divided into three stages. In the first stage, the spherical particles are squeezed by the detonation wave, and the windward side shell cracks. During the second stage, the particle rebounds, the shell breaks and is peeled by the detonation product stripping with internal aluminum core stress, and the internal aluminum steam burns with the detonation products. For the third stage, the detonation product alumina cannot be attached

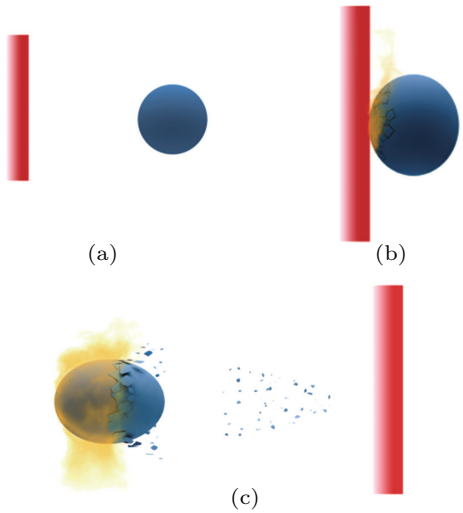


Fig. 9. The structural response diagram of aluminum particle in detonation environment.

to the surface of the core, so the aluminum keeps evaporating and burning with some product being attached to the container wall and some condensing into sub-micron particle clusters. The structural response of aluminum particle is shown in Fig. 9.

5. Conclusions

The analysis of the aluminum particle product for detonation environments demonstrates that the aluminum particle burns in a gaseous state and condenses into a sub-micron particle cluster.

The rupture of the aluminum particle shell in the detonation environment is mainly caused by the impact of the detonation wave. The result shows that the detonation wave impacts on the aluminum particles, resulting in shell cracking and then, due to the shrinkage-expansion of the aluminum core and stripping of the detonation products, the cracked shell is fractured and peeled with the aluminum reacting with the detonation product.

The core–shell structure response of the aluminum particle in a detonation environment provides a foundation for studying the combustion behavior and revealing the burn mechanism of aluminum particles in such environments.

References

[1] Keshavarz M H 2005 *Combust. Flame* **142** 303
[2] Peuker M, Krier H and Glumac N 2013 *Proc. Combust. Inst.* **34** 2205
[3] Ruggirello K P, DesJardin P E, Baer M R, Kaneshige M J and Hertel E S 2012 *Int. J. Multiphase Flow* **42** 128
[4] Keicher T, Happ A, Kretschmer A, Sirringhaus U and Wild R 1999 *Propellants Explos. Pyrotech* **24** 140
[5] Firmansyah D A, Sullivan K, Lee K S, Kim Y H, Zahaf R, Zachariah M R and Lee D 2011 *J. Phys. Chem. C* **116** 404
[6] Eisenreich N, Fietzek H, Juez-Lorenzo M, Kolarik V, Koleczko A and Weiser V 2004 *Propellants Explos. Pyrotech* **29** 137
[7] Hasani S, Panjepour M and Shamanian M 2012 *Oxidation Met.* **78** 179
[8] Hasani S, Panjepour M and Shamanian M 2014 *Oxidation Met.* **81** 299
[9] Korshunov A V, Il'In A P, Radishevskaya N I and Morozova T P 2010 *Russ. J. Phys. Chem. A* **84** 1576
[10] Eisenreich N, Fietzek H, Juez-Lorenzo M, Kolarik V, Weiser V and Koleczko A 2005 *High Temp.* **22** 329
[11] Dreizin E L 1996 *Combust. Flame* **105** 541
[12] Trunov M A, Schoenitz M and Dreizin E L 2005 *Propellants Explos. Pyrotech.* **30** 36
[13] Trunov M A, Schoenitz M, Zhu X and Dreizin E L 2005 *Combust. Flame* **140** 310
[14] Trunov M A, Schoenitz M and Dreizin E L 2006 *Combust. Thero. Model* **10** 603
[15] Levin I and Brandon D 2005 *J. Am. Ceram. Soc.* **81** 1995
[16] Brandstadt K, Frost D L and Kozinski J A 2009 *Proc. Combust. Inst.* **32** 1913
[17] Liu Y, Ren H and Jiao Q J 2017 *IOP Conf. Ser.: Mater. Sci. Eng.* **248** 012002
[18] Glassman I 1959 *Metal Combustion Processes*, American Rocket Society Preprint, New York
[19] Brzustowski T A, Glassman I 1964 *Heterogeneous Combustion*, (New York: Academic Press)
[20] Law C K 1973 *Combust. Sci. Technol.* **7** 197
[21] Brooks K P and Beckstead M W 1995 *J. Propul. Power* **11** 769
[22] Olsen S E and Beckstead M W 1996 *J. Propul. Power* **12** 662
[23] Allen D, Krier H and Glumac N 2014 *Combust. Flame* **161** 295
[24] Lokenbakh A K, Zaporina N A, Knipele A Z, Strod V V and Lepin L K 1985 *Combust. Explo. Shock* **21** 69
[25] Boiko V M, Lotov V V and Papyrin A N 1989 *Combust. Explo. Shock* **25** 193
[26] Rozenb, V I and Vaganova N I 1992 *Combust. Flame* **88** 113
[27] Zhang S and Dreizin E L 2013 *J. Phys. Chem.* **117** 14025
[28] Nie H, Zhang S, Schoenitz M and Dreizin E L 2013 *Int. J. Hydrogen Energy* **38** 11222
[29] Shang J F and Zheng F Y 1991 *Lang's Handbook of Chemistry* (Translated version) (Beijing: Science Press) p. 72 (in Chinese)
[30] Sun Y B, Hui J M and Cao X M 1995 *Military Mixed Explosive* (Beijing: Publishing House of Ordnance Industry) p. 96 (in Chinese)
[31] Sućeska M 2015 *Explo5 Program* (version 6.03), Zagreb
[32] Lee E L, Hornig H C and Kury J W 1968 "Adiabatic Expansion of High Explosive Detonation Products", Report Published by Lawrence Radiation Laboratory
[33] Dieter G E and Bacon D J 1986 *Mechanical metallurgy* (New York: McGraw-hill) p. 53
[34] Holmquist T J, Johnson G R, Lopatin C M, Grady D E and Hertel E S 1995 "High strain rate properties and constitutive modeling of glass", Report published by Sandia National Laboratories